PAPER

Visible sequestration of Cu²⁺ ions using amino-functionalized cotton fiber

Changkun Liu,* Xiaobin Lei, Xiaoyan Liang, Jizhen Jia and Lin Wang

In this study, an amino functionalized cotton fiber, which was used to adsorb Cu²⁺ ions *via* visible sequestration, was prepared and investigated. The amino-functionalized cotton fiber (named as ACF) exhibited enhanced adsorption, selectivity and distinct color response to Cu²⁺ ions in aqueous solutions. The absorbance responses of ACF to Cu²⁺ ions (named as ACF–Cu), obtained from the a fiber optic spectrometer, were monitored with different pH values and initial Cu²⁺ ion concentrations. A linear relationship between the absorbance response and the initial concentrations of Cu²⁺ ions was established and can be used for the determination of Cu²⁺ ion concentrations in aqueous solutions. Furthermore, in the interference study, ACF showed great selectivity to Cu²⁺ ions when other ions (*e.g.*, Pb²⁺ or Zn²⁺ ions) coexisted with the Cu²⁺ ions in solution. The ability of ACF to effectively detect Cu²⁺ ions with the presence of other interfering ions in solution was of great significance.

1. Introduction

The rapid industrial development of petroleum refining, metallurgical mining, electro-plating and chemical manufacturing has led to large quantities of discharged wastewater containing heavy metal ions.[1] Heavy metal ions are not only toxic and non-degradable, but also able to be accumulated in human body and natural environment. Excessive intake of heavy metal ions, such as copper ions, may cause serious damage to nervous and urinary systems.[2] Therefore, many methods have been used for the removal of copper ions from wastewaters, including chemical precipitation, chemical reduction, electrochemical treatment, ion exchange and adsorption.[3] Among these methods, adsorption has become an advantageous technique due to its low cost, great adsorption capacity, good selectivity and reusability. Yantasee *et al.* prepared nitro groups modified active carbon and then reduced them to amino groups for adsorbing Cu²⁺ ions with 0.86 mmol g⁻¹ adsorption capacity.[4]

The adsorbents usually adsorb heavy metal ions through the interactions of the functional groups on the adsorbents' surface with the heavy metal ions.[5] Therefore, the functional groups of the adsorbents are important for the adsorption performances. Currently, the amine group is regarded as one of the most effective groups for heavy metal ions adsorption due to the high affinity of the formed amine–metal complex on the adsorbent surface.[6–8] For instance, Yang *et al.* synthesized cyclic diamine-grafted chitosan-crown ether, which showed great selectivity for

Cu²⁺ ion adsorption when Pb²⁺, Cu²⁺ and Cd²⁺ ions co-existed in the solution.[9]

Copper ion can hardly be observed in aqueous solutions due to its colorless and odorless nature when its concentration is relatively low. Traditional copper ion concentration determination methods include visible spectrophotometry, atomic absorption, electrochemical analysis, fluorescence spectrometry and inductively coupled plasma mass spectrometry, *etc.* However, most of these methods need complicated sample preparation process, large instruments and high expenses,[10,11] which are not suitable for on-site detection. Besides, it is favorable and imperative to accomplish both the on-site convenient detection and efficient removal of copper ions in a simultaneous manner. Therefore, a low-cost, easy-to-use, and small-size device is extremely needed for monitoring and removing copper ions. In recent years, the stable colorimetric strategies have attracted more and more attention for easy detection of a certain heavy metal ion *via* the color changes. For example, Liu *et al.* had prepared a porphyrin-functionalized polyacrylonitrile fiber as the highly selective and sensitive colorimetric mercury sensor for mercury ions detection.[12] However, it is of great value if both functions of detection and adsorption towards the target heavy metal ion be combined onto one material, so as to provide the early warning and efficient removal of the heavy metal ions.

In recent years, cotton fiber as one of the cheap and abundant biomaterials, which are mainly composed of cellulose, has attracted much research attention. Cotton fiber can be surface modified due to the hydroxyl groups present on the cellulose.[13–15] For example, Monier *et al.* reported a modified cotton fiber prepared *via* the graft polymerization and surface modification methods, which was used to adsorb Au³⁺, Pd²⁺ and Ag⁺ ions in

Shenzhen Key Laboratory of Environmental Chemistry and Ecological Remediation, College of Chemistry and Environmental Engineering, Shenzhen University, 3688 Nanhai Ave., Shenzhen, 518060, Guangdong Prov., P. R. China. E-mail: liuck@szu.edu.cn

aqueous solutions and showed the highest adsorption capacity for Au^{3+} ion.[16] Although cotton fiber can be modified for various applications, the multi-functions of copper ion adsorption and detection with the aminated cotton fiber (named as ACF) through chromogenic reaction have seldom been reported before. The ACF samples would reflect the environment-friendly significance through the monitoring and control of copper ions in the solution. In addition, the use of the modified cotton fiber materials demonstrates the great strategic awareness favorable to both economy and environment. In this study, the cotton fiber was used as the substrate, and the glycidyl methacrylate (GMA) was polymerized and grafted onto the cotton fiber (as PGMA polymer brush) *via* the surface-initiated atom transfer radical polymerization (SI-ATRP) technology. Then, diethylenetriamine (DETA) was immobilized onto PGMA polymer brushes through the ring-opening reaction. The prepared multi-functional cotton fiber was examined for its color change properties in response to copper ions, as well as the adsorption performances towards the copper ions in aqueous solutions.

2. Experimental

2.1 Materials

Cotton fibers were provided by Qingbai Plastic Products Factory. 2-Bromoisobutyryl bromide (BIBB, AR, 98%), cobalt nitrate hexahydrate (AR, 99%), iron(II) chloride tetrahydrate (AR, 99%), nickel nitrate hexahydrate (AR, 98%), copper nitrate tetrahydrate (AR, 99%), copper(II) bromide ($CuBr_2$, 99%), glycidyl methacrylate (GMA, AR, >97%), N,N-dimethylformamide (DMF, AR, 99.5%), tetrahydrofuran (THF, AR, 99%), copper(I) bromide (CuBr, AR, 99%), 2,2′-bipyridyl (Bpy, AR, >99%) and EDTA (disodium salt-ethylene diamine tetraacetic acid, 0.1 mol L^{-1}) were purchased from Shanghai Aladdin Reagent Co., Ltd. Dichloromethane (DCM, AR), sodium hydroxide (NaOH, AR), acetone (AR) and methanol (AR, 99.9%) were purchased from Tianjin Baishi Chemical Company.

2.2 Preparation of the aminated cotton fiber

Firstly, 1 g pristine cotton fiber and 30 mL DCM were added into the test tube, in which 10 mL BIBB and 1 mL pyridine were added slowly. The mixtures in the test tube were stirred at the stirring speed of 150 rpm on a magnetic stirrer for 24 h in an ice-water bath to prepare the brominated cotton fiber. After the reaction, the brominated cotton fiber (denoted as cotton-Br) was taken out, repeatedly rinsed with acetone and deionized water, and then dried in a dry box. Secondly, SI-ATRP technology was used to graft PGMA polymer brushes on the surface of the cotton-Br. 0.5 g cotton-Br was placed in a test tube, in which 5 mL deionized water, 10 mL DMF, 15 mL GMA, 0.5 g Bpy, 0.1 g CuBr and 0.05 g $CuBr_2$ were added. The reaction was carried out for 2 h at 45 °C under argon atmosphere to produce PGMA-grafted cotton fiber (denoted as cotton-PGMA). The obtained cotton-PGMA was then washed with THF, acetone, 0.1 M EDTA and deionized water, in that sequence, and dried in a dry box. Thirdly, 0.1 g of the prepared cotton-PGMA was put in a test tube, in which 5 mL THF and 5 mL diethylenetriamine (DETA)

were added for the amination reaction at room temperature at the stirring speed of 150 rpm for 24 h to prepare the aminated cotton fiber (ACF). Finally, the ACF was washed with acetone and deionized water, and dried in a dry box for future use.

2.3 Characterization

The functional group characterization of the cotton fiber samples was examined using Fourier Transform Infrared Spectrometer (FTIR-8300PCS, Shimadzu, Japan). The surface morphologies of the cotton fiber samples were observed with Scanning Electron Microscope (SEM) (S-3400N, Hitachi, Japan). The surface element recognition of the cotton fiber samples was examined with X-ray Photoelectron Spectroscopy (XPS, Thermo ESCALAB 250Xi, USA).

2.4 Adsorption and detection performances

The copper ion adsorption experiments were carried out with the ACF as the adsorbents. All the experiments were conducted in beakers at 25 °C at the stirring speed of 150 rpm for 12 h. The copper ion concentrations before and after the adsorption process were measured by the Inductively Coupled Plasma Optical Emission Spectrometer (ICP-OES, Optima 2100DV, PerkinElmer). The copper ion adsorption capacity was calculated according to eqn (1):

$$q = \frac{(C_0 - C) \times V}{m} \tag{1}$$

where q (mmol g^{-1}) is the adsorption capacity, C_0 and C (mmol L^{-1}) are the copper ion initial and final concentrations in solution, respectively, V (L) is the volume of the copper ion solution, and m (g) is the weight of the adsorbents. The color changes of the copper ion-adsorbed ACF (denoted as ACF–Cu) were recorded by taking digital photographs of the ACF–Cu after the adsorption process with the specific adsorption conditions.

For the pH effect on copper ion adsorption, each of the 50 mg ACF were placed in a series of 4 mmol L^{-1} copper nitrate solutions (50 mL each, pH adjusted to 1–5). Copper ions (in Cu^{2+} form) are the predominant species under such adsorption conditions, as determined by the MINEQL+ software.[17] Finally, the copper ion-adsorbed ACF (ACF–Cu) were taken out, rinsed with deionized water and measured by the fiber optic spectrometer (MAX2000-Pro, Wenyi, Shanghai) for absorbance determination. The derived absorbance responses of ACF–Cu were monitored and recorded.

For the adsorption kinetics experiments, 500 mg ACF was decanted into 500 mL of 4 mmol L^{-1} copper nitrate solution at pH 5. Samples were taken at the designated time intervals in the adsorption process and the concentration of the samples was measured by ICP-OES.

For the adsorption isotherm experiments, 50 mg ACF each were decanted into a series of 50 mL copper nitrate solutions at pH 5 with concentrations ranging from 0.1 to 4 mmol L^{-1}. After the adsorption equilibrium was reached, the ACF–Cu were taken out, rinsed with deionized water and examined for the absorbance with the fiber optic spectrometer.

To examine the effect of the interfering ions, the adsorption was conducted with ACF in the solutions at pH 5 containing

1 mmol L^{-1} copper ions and 1 or 4 mmol L^{-1} other ions, including Na$^+$, Zn^{2+}, Fe^{2+}, Co^{2+}, Ni^{2+} and Pb^{2+} ions. After the adsorption process, the cotton fiber samples were taken out, rinsed with deionized water and examined for the absorbance with the fiber optic spectrometer.

2.5 Desorption and repeated use studies

In the desorption study, the ACF–Cu sample (derived from the adsorption process: 50 mg ACF, 50 mL of 4 mmol L^{-1} copper nitrate solution, pH 5) each were placed into 50 mL HNO$_3$ with the concentration range of 0.01–2.00 mol L^{-1} for the desorption of copper ions. The desorption efficiency was calculated using the following equation:[18]

$$DE = \frac{C_{el}V}{q_{el}m} \times 100\% \qquad (2)$$

where q_{el} (mmol g^{-1}) is the amount of copper ions adsorbed on the adsorbents before the desorption experiment, C_{el} (mmol L^{-1}) is the copper ion final concentrations in HNO$_3$ solution after the desorption process, V (L) is the volume of the HNO$_3$ solution, and m (g) is the weight of the ACF adsorbent.

In the repeated use study, 200 mg ACF was first put into 200 mL of 4 mmol L^{-1} copper nitrate solution at pH 5 for copper ion adsorption. Then, the derived ACF–Cu was put into 200 mL of 0.5 mol L^{-1} HNO$_3$ solution for the desorption of copper ions, followed by 0.5 mol L^{-1} NaOH solution wash for 30 min for regeneration and repeated water wash until the pH of the washing water became neutral. After that, the regenerated ACF was again used for copper ion adsorption and the adsorption–desorption–regeneration process was repeated for 6 cycles. The desorption efficiency and adsorption capacity of the ACF during the 6 cycles were recorded.

3. Results and discussion

3.1 Functionalization of the cotton fiber

The synthesis route of the ACF sample was shown in Fig. 1. BIBB reacted with the hydroxyl groups of the cotton fiber to produce the cotton-Br, which acted as the macro initiator for the subsequent PGMA polymerization via the SI-ATRP technique. The subsequently derived cotton-PGMA was further reacted with DETA via the ring-opening reaction for the immobilization of DETA, and the ACF sample was derived.

3.2 Characterization of cotton fibers

The surface morphologies of the cotton fiber in different preparation stages were observed using SEM. As shown in Fig. 2(a), the surface of the pristine cotton was relatively smooth. After the bromination, the surface of cotton-Br in Fig. 2(b) showed almost no obvious changes. The surface morphologies of cotton-PGMA and ACF were shown in Fig. 2(c) and (d), respectively. It can be observed that significant changes occurred as the surface was much rougher, indicating that the surface grafting of PGMA and the subsequent immobilization of DETA were prone to change the surface morphologies of the cotton fibers.
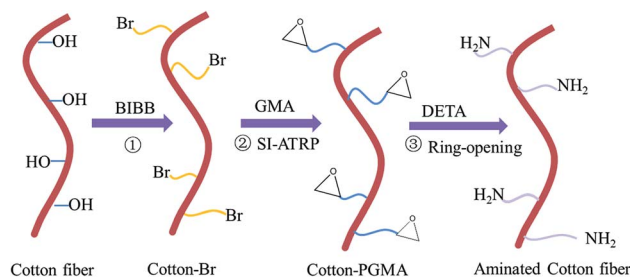

Fig. 1 Schematic diagram of the preparation process of the aminated cotton fiber (ACF).

The polymeric loading capacity of PGMA of the cotton fiber was determined by the examination of the grafting yield (GY), which was defined as GY $= \dfrac{W_b - W_a}{W_a}$, where W_a and W_b were the weights of the brominated cotton fiber (cotton-Br) before and after surface grafting of PGMA polymers, respectively. The derived GY value was 5.55%. The amine loading yield (AY) in the amination process was similarly defined as AY $= \dfrac{m_b - m_a}{m_a}$, where m_a and m_b were the weights of the PGMA-grafted cotton fiber (cotton-PGMA) before and after amination reaction with DETA, respectively. The derived AY value was 3.67%.

Fig. 3 showed the FTIR spectra of the cotton fiber samples during the preparation procedures. The broad peak at 3325 cm^{-1} was characteristic for the hydroxyl groups of the pristine cotton.[19] After the bromination, the C=O stretching vibration peak appeared at 1730 cm^{-1} in Fig. 3(b), indicating the successful introduction of BIBB onto the pristine cotton.[20] For the spectrum of cotton-PGMA in Fig. 3(c), new peaks appeared at 1147 cm^{-1} and 1260 cm^{-1} for the symmetric and asymmetric vibration of the C–O group in GMA molecules, respectively, and at 906 cm^{-1} and 845 cm^{-1} for the vibration absorption of the epoxy group, indicating that PGMA polymer brush was successfully immobilized on cotton-Br.[21] For the spectrum of the ACF sample in Fig. 3(d), a broad peak appeared in the range of 3100–3700 cm^{-1}, which was contributed by the stretching vibration of both the hydroxyl and amine groups. The new peak at 1160 cm^{-1} for C–N stretching vibration and at 967 cm^{-1} for N–H wag vibration, together with the disappearance of the epoxy group characteristic peaks all indicated the successful amination of the cotton fiber to produce the ACF.[22]

XPS was used to examine the surface chemical composition of the cotton fiber samples, as shown in Fig. 4. The peaks of C 1s and O 1s appeared in the pristine cotton wide scan spectrum in Fig. 4(a). The C 1s core-level spectrum of the pristine cotton was further sub-divided into three peaks at the binding energies of 284.6, 286.2 and 287.7 eV, attributing to the C oxidation states in C–C/C–H, C–O and O–C–O, respectively, indicating presence of the cellulose in pristine cotton.[23] In Fig. 4(c), new peaks were observed (for Br 3d and Br 3p), indicating the successful introduction of BIBB to form cotton-Br. Likewise, four peaks were sub-divided for the C 1s core-level spectrum in Fig. 4(d) at the binding energies of 284.6, 286.2, 287.7 and 288.8 eV, and the new peak at 288.8 eV indicated the presence of
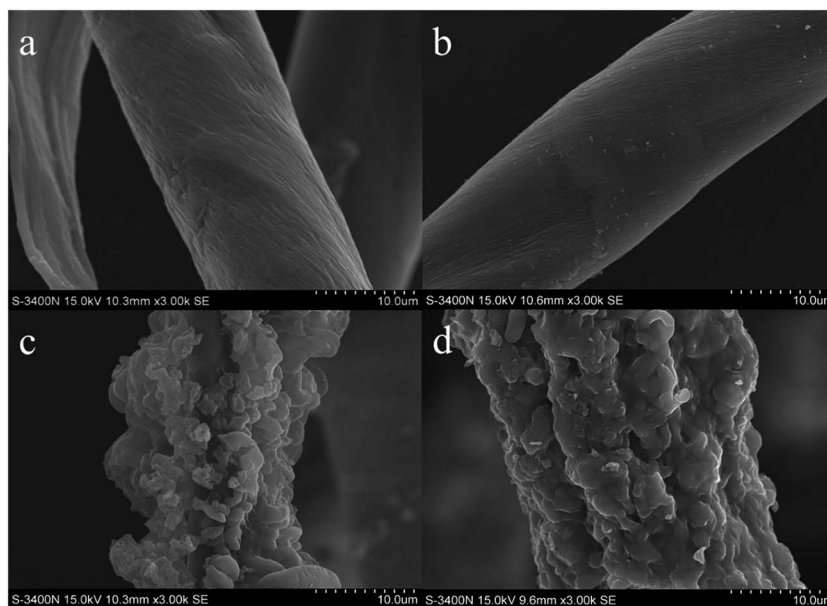
Fig. 2 SEM images of the cotton fibers before and after modification: (a) pristine cotton fiber; (b) cotton-Br; (c) cotton-PGMA; (d) aminated cotton fiber (ACF).
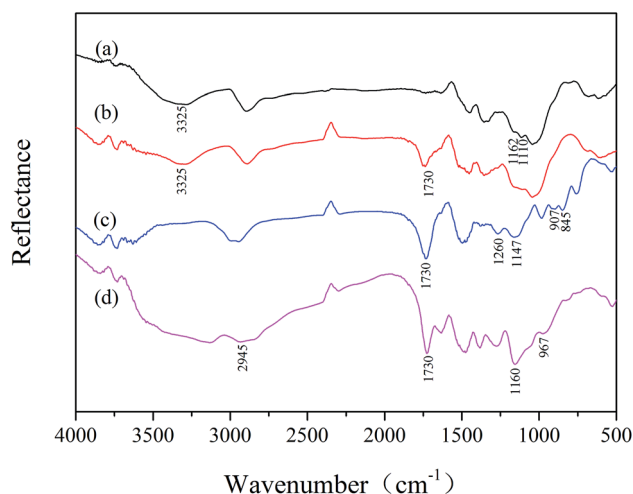

Fig. 3 FTIR spectra of the (a) pristine cotton; (b) cotton-Br; (c) cotton-PGMA and (d) aminated cotton fiber.

the O–C=O groups in the immobilized BIBB groups on cotton-Br.[24] After the amination reaction, N 1s peak appeared in the XPS wide scan spectrum of ACF in Fig. 4(e). The N 1s core-level spectrum was subsequently sub-divided into two peaks in Fig. 4(f) at the binding energies of 398.9 and 400.9 eV, corresponding to the nitrogen in neutral amine and protonated amine groups, respectively.[25] After copper ion adsorption with the ACF, the C 1s, O 1s, N 1s and a new peak Cu 2p appeared in the wide scan spectrum of ACF–Cu (Fig. 4(g)). The N 1s core-level spectrum of ACF–Cu was sub-divided into four peaks at the binding energies of 399, 399.7, 401.2 and 406.5 eV. Compared with Fig. 4(f), the new peak at 399.7 eV was attributed to the N element of the copper ion-coordinated amine, due to

the electron-donating nature of the N element in the ACF–Cu coordination.[26] The peak at 406.5 eV was attributed to the N element of the NO_3^- groups, which was present on the surface of ACF–Cu to balance the positive charges of the adsorbed copper ions and make the ACF–Cu in a neutral state.

3.3 Visible sequestration of copper ions

The effect of pH values was investigated on the copper ion adsorption and detection performances. The absorbance (at 458 nm), adsorption capacity and the color changes of the ACF samples in response to copper ions with pH values range from 1 to 5 were shown in Fig. 5.

It was shown that both the absorbance of ACF–Cu and the adsorption capacity of ACF sample showed an increase with the increase of the pH value. At low pH value, the H^+ with much higher concentration than the copper ions competed for the amine sites on ACF samples in solution, resulting in the protonated amines, which in turn prevented the approaching of copper ions through the strong electrostatic repulsion.[27] It was observed from Fig. 5 that the ACF–Cu at pH 1 showed a while color with a small amount of copper ions adsorbed. The small amount of the adsorption capacity achieved at pH 1 was probably due to the physical adsorption of copper ions on the ACF. As the blue color was due to the formation of the amine–Cu complex on ACF–Cu, the white color of ACF–Cu at pH 1 indicated the strong protonation effect of amine sites which prevented the coordination of copper ions with ACF. Therefore, the white color of ACF–Cu at pH 1 was similar with the color of the ACF at 0.1 M HNO_3 solution (protonated ACF at pH 1) (data not shown). As the pH increased, the effects of both the amine protonation and the electrostatic repulsion were decreased. As a result, the copper ion adsorption capacity showed an increase, with the formation of the amine–Cu complex, which resulted in
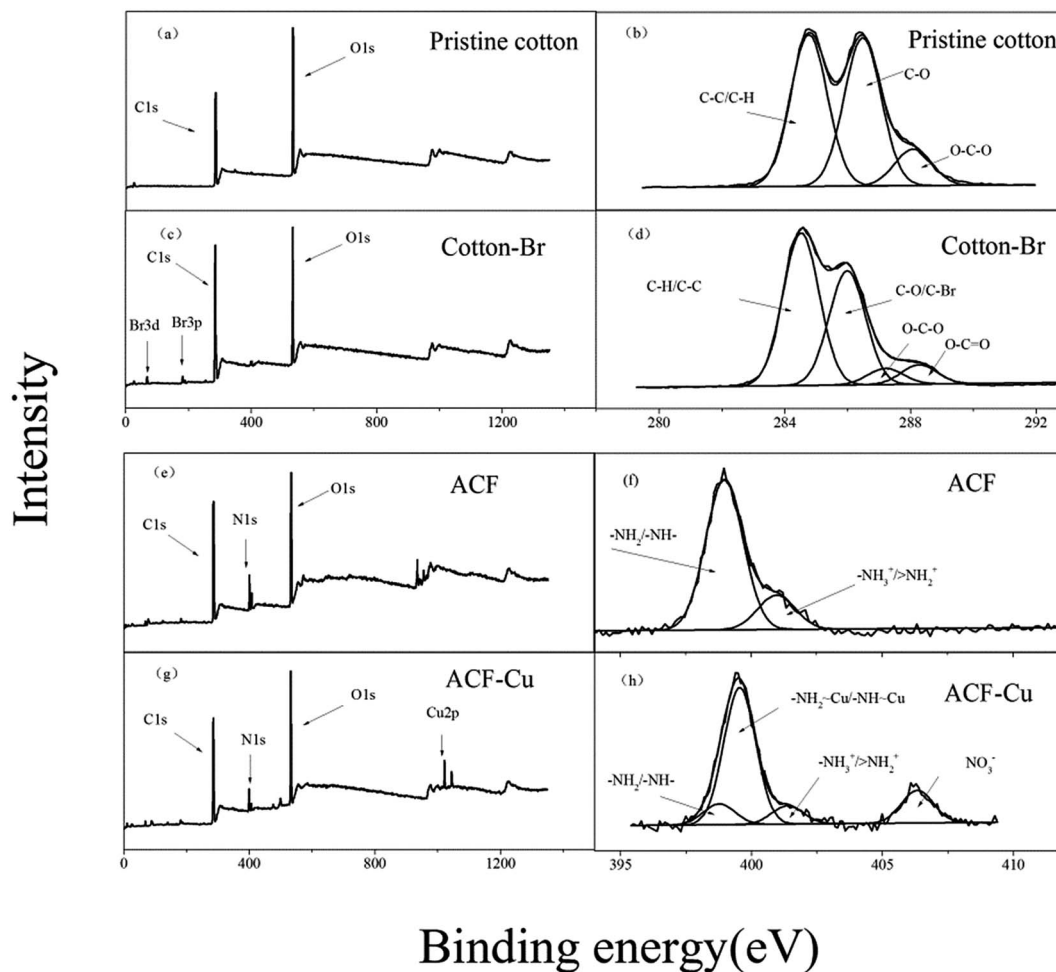
Fig. 4 XPS wide scan spectra of (a) pristine cotton; (c) cotton-Br; (e) ACF and (g) ACF–Cu; C 1s spectra of (b) pristine cotton and (d) cotton-Br, and N 1s spectra of (f) ACF and (h) ACF–Cu.
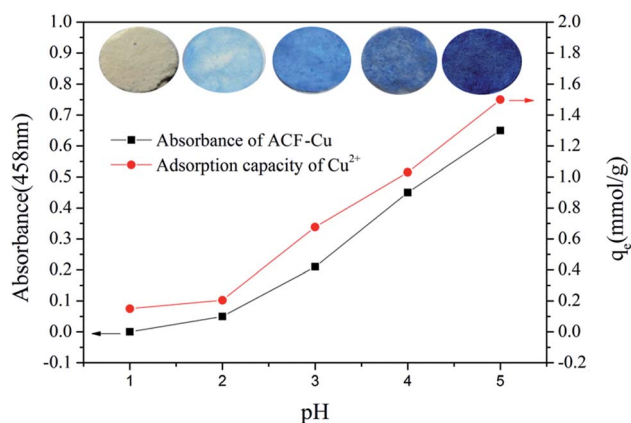

Fig. 5 Absorbance (at 458 nm wavelength), adsorption capacity and color change of the ACF samples in response to copper ion solutions at different pH values.

the blue color of the ACF–Cu. Therefore, the color of the ACF–Cu turned from white (at pH 1) to blue (at pH > 2), and the reflectance intensity can be detected at 458 nm wavelength. The

ACF samples could be used at the solution pH of 5 for better sensitivity and good adsorption capacity.

The reflectance spectra of the ACF–Cu after copper ion adsorption with different initial copper ion concentrations ranging from 0.1–1.0 mmol L^{-1} were shown in Fig. 6(a). It could be seen that the strong reflectance intensity at 458 nm wavelength appeared, which was attributed to the blue color of ACF–Cu. The intensity of the reflectance spectra of the ACF–Cu clearly decreased as the copper ion initial concentration increased. At the meantime, it could be easily observed in the inset figure in Fig. 6(b) that the color of the ACF–Cu changed from light blue to dark blue as the concentration of copper ion increased from 0.1 mmol L^{-1} to 1.0 mmol L^{-1}. Based on the derived result, a linear relationship was established for the absorbance *versus* the initial copper ion concentrations, with the linear fitting correlation coefficient R^2 of 0.9962. Therefore, a simple and fast method for copper ion concentration determination was established using the derived linear relationship as the detection criterion. Compared with the traditional heavy metal ion concentration determination methods, this method presented much convenience in detection with the ACF sample.
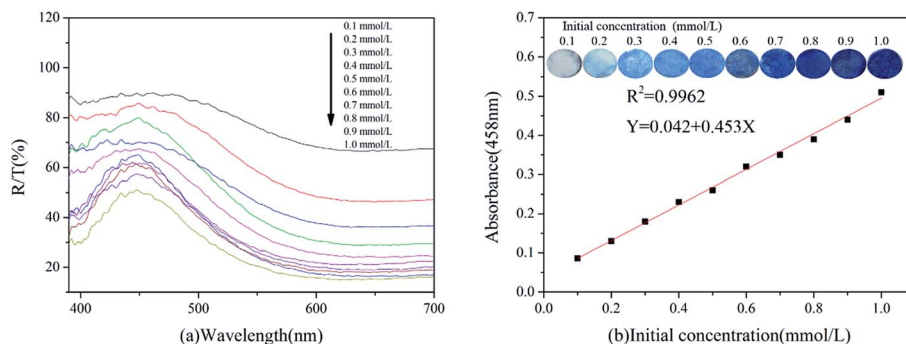
Fig. 6 (a) The reflectance spectra of ACF−Cu samples after copper ion adsorption in solution with different copper ion initial concentrations; (b) the linear fit of the absorbance data *versus* the initial concentrations of copper ion, with the inlet pictures of the ACF−Cu samples after copper ion adsorption in solutions with different copper ion initial concentrations.
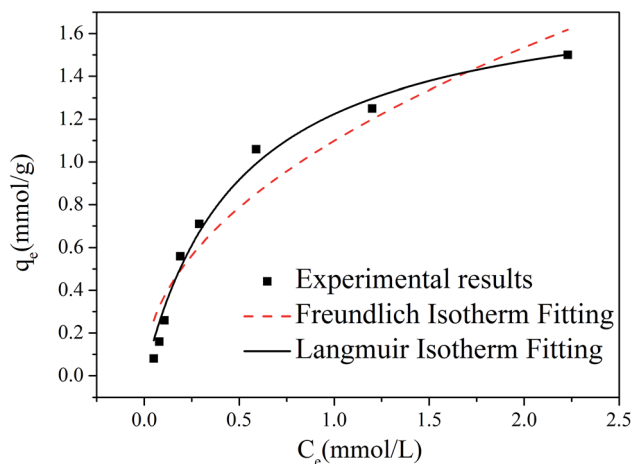

Fig. 7 Copper ion adsorption isotherm with ACF samples at pH 5.

Besides, the copper ion concentration determination with the portable fiber optic spectrometer was easy in operation, which had practical application prospect in the field of emergent environmental monitoring and the wastewater treatment.

3.4 Adsorption performances

The copper ion adsorption isotherm with ACF samples was shown in Fig. 7. The experimental data were fitted with Langmuir and Freundlich isotherm models. The Langmuir model assumed a homogeneous surface for the adsorption, with a monolayer of the adsorbed substance. The Langmuir isotherm model equation was expressed as follows:

$$q_e = \frac{b_L q_m C_e}{1 + b_L C_e} \tag{3}$$

where q_e (mmol g^{-1}) and C_e (mmol L^{-1}) were the equilibrium adsorption capacity and copper ion equilibrium concentrations in the solution, respectively. q_m (mmol g^{-1}) was the maximum adsorption capacity as derived from the Langmuir model, and b_L was the Langmuir model constant (L mmol^{-1}) reflecting the affinity between the adsorbate and the absorbent.

The Freundlich model assumed a heterogeneous surface for the adsorption with multi-layer adsorbates on the surface. The Freundlich isotherm model equation was expressed as follows:

$$q_e = b_F C_e^{1/n} \tag{4}$$

where C_e and q_e were defined above, b_F (mmol$^{1-1/n}$ L$^{1/n}$ g^{-1}) was the Freundlich model constant, and $1/n$ was a constant indicating the adsorption intensity.

The fitting results to the experimental data with the Langmuir and Freundlich isotherm models were shown in Fig. 7, with the calculated model parameters listed in Table 1. It could be seen that the Langmuir isotherm model fitted the data better with the correlation coefficient (R^2) of 0.9815, which indicated a monolayer coverage on the ACF sample surface. The q_m was derived to be 1.84 mmol g^{-1}, indicating a good adsorption performance with great potentials for the treatment of heavy metal ions. The high adsorption capacity of copper ions on ACF sample would be attributed to the abundant amine groups on the surface of the ACF.

The copper ion adsorption kinetic behaviors with the ACF samples at different copper ion initial concentrations were shown in Fig. 8. Generally, the copper ion adsorption showed an

Table 1 Parameter values from the adsorption isotherm models fitting to the experimental results in Fig. 7 for copper ion adsorption on ACF samples at pH 5

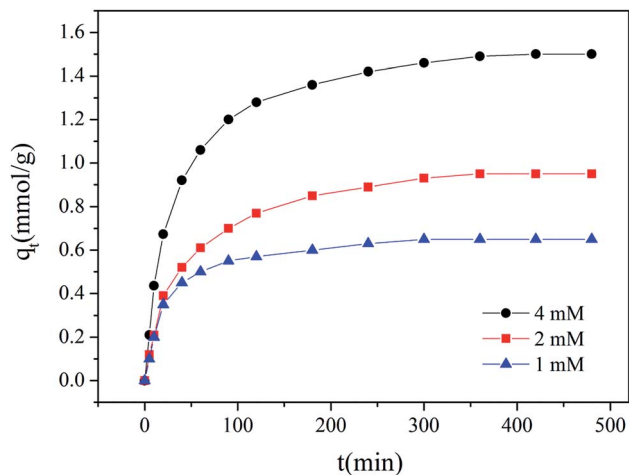| Langmuir			Freundlich		
q_m (mmol g^{-1})	b_L (L mmol^{-1})	R_L^2	b_F (mmol$^{1-1/n}$ L$^{1/n}$ g^{-1})	n	R_F^2
1.84	1.9783	0.9815	1.0989	2.0730	0.9122

Fig. 8 Copper ion adsorption kinetics with the ACF samples at different copper ion initial concentrations at pH 5.

initial sharp increase, followed by a steady plateau, with the increase of the adsorption time. In addition, the adsorption capacity of copper ions clearly increased with the increase of the initial copper ion concentrations. The results indicated that the amine binding sites for copper ions were abundant, and stronger driving force for mass transfer and the subsequent surface adsorption occurred at higher copper ion concentrations.[28] In order to analyze the adsorption kinetics for copper ions, the pseudo-first-order (PFO) and pseudo-second-order (PSO) kinetic models were applied to fit the experimental data. The two kinetic equations were shown as follows:

$$\ln(q_e - q_t) = -k_1 t + \ln q_e \quad (5)$$

$$\frac{t}{q_t} = \frac{t}{q_e} + \frac{1}{k_2 q_e^2} \quad (6)$$

where q_t (mmol g^{-1}) was the adsorption capacity at time t (min) during adsorption, q_e (mmol g^{-1}) was the adsorption capacity at the adsorption equilibrium, k_1 (min^{-1}) was the rate constant of the PFO kinetics model, and k_2 (g (mmol^{-1} min^{-1})) was the rate constant of PSO kinetics model.

The model parameters derived from the fitting of the experimental data were summarized in Table 2. Experiment results suggested that the PSO model provided the best fitting of the experimental data with the correlation coefficient R^2 of 0.9937–0.9996, which was higher than those of the PFO model. Furthermore, the values of q_e obtained from the PSO model were in good agreement with the experimental data. Thus, the good fitting of the PSO model to the copper ion adsorption kinetics indicated

that the adsorption of copper ion on ACF sample was dominated by chemical adsorption, in which the surface amine groups coordinated with copper ions through sharing the lone pair electrons of the nitrogen element in amine groups.

3.5 Interference experiments

The interference on the adsorption and detection of copper ions with ACF samples was investigated when Na$^+$, Pb^{2+}, Fe^{2+}, Co^{2+}, Ni^{2+} and Zn^{2+} ions as the interfering ions coexisted with Cu^{2+} ions in solution. The distribution constant (K_d), which was used to express the stability of metal–ligand complex, was calculated for both copper ion and other interfering ions.[29] A higher K_d value usually indicated a more stable metal–ligand complex.[30] The K_d was calculated according to the following eqn (7) and listed in Table 3.

$$K_d = \frac{C_0 - C_e}{C_e} \frac{V}{m} \quad (7)$$

where C_0, C_e, V and m are defined before. As shown in Table 3, the copper ion adsorption capacity of the ACF sample showed almost no changes when Na$^+$, Pb^{2+}, Fe^{2+} and Zn^{2+} ions were present in solution with the copper ions, indicating a good adsorption selectivity of ACF for copper ions. However, Co^{2+} and Ni^{2+} ions did have some influences on the adsorption of copper ions with ACF. It could be seen that the K_d of ACF–Cu was much higher than other heavy metal ion-coordinated ACF samples, indicating that the affinity of ACF samples toward Cu^{2+} ions was much higher than those towards the Fe^{2+}, Co^{2+}, Ni^{2+}, Zn^{2+} and Pb^{2+} ions. Therefore, the ACF samples showed good adsorption selectivity towards Cu^{2+} ions. Besides, the blue color of the ACF–Cu and the corresponding absorbance shown in Table 3 were almost not affected by most of the interfering ions investigated in this study except Co^{2+} and Ni^{2+} ions. Even when the concentration of the Fe^{2+}, Zn^{2+} and Pb^{2+} ions was 4 times that of Cu^{2+} ions, the adsorption capacity and the absorbance still remained almost the same as compared with those when only Cu^{2+} ions were present during adsorption.

According to the Irving-Williams sequence,[31] the stability of the complex of metal ion and nitrogen-contained ligand was in the order of Mn^{2+} < Co^{2+} < Fe^{2+} < Pb^{2+} < Ni^{2+} < Cu^{2+} > Zn^{2+}, indicating that the complex of the amine group with Cu^{2+} ions was more stable. Furthermore, the stability constants (in log K form) of the metal–DETA complex were listed in Table 4. The log K of Cu–DETA complex was much higher than that of Pb–DETA, Fe–DETA, Co–DETA, Ni–DETA and Zn–DETA complex, indicating the selective adsorption ability of the DETA immobilized on the ACF surface to Cu^{2+} ions in the solution when other interfering ions were present.

Table 2 Parameter values of the kinetics models fitting to the experimental data in Fig. 8 for copper ion adsorption on ACF at pH 5

Cu^{2+}	Pseudo-first-order (PFO) model		Pseudo-second-order (PSO) model		
C_0 (mmol L^{-1})	k_1 (min^{-1})	R_1^2	q_e (mmol g^{-1})	k_2 (g (mmol^{-1} min^{-1}))	R_2^2
4	0.0085	0.9736	1.5750	0.0160	0.9937
2	0.0118	0.9868	1.0380	0.0263	0.9995
1	0.0135	0.9503	0.6872	0.0401	0.9996

Paper

RSC Advances

Table 3 Adsorption capacity of ACF sample and the corresponding color of ACF–Cu after copper ion adsorption in the presence of other interfering ions in the solutions at pH 5

Metal ions	Concentration ratio	Cu^{2+} uptake (mmol g^{-1})	Color of ACF–Cu	Absorbance (at 458 nm)	K_d (L g^{-1})
Cu^{2+}	—	0.700		0.46	2.45
Na^+/Cu^{2+}	4 : 1	0.723		0.46	2.85
Zn^{2+}/Cu^{2+}	1 : 1	0.703		0.47	0.08/2.45
	4 : 1	0.683		0.45	0.11/2.65
Pb^{2+}/Cu^{2+}	1 : 1	0.703		0.47	0.05/2.43
	4 : 1	0.700		0.46	0.003/1.60
Ni^{2+}/Cu^{2+}	1 : 1	0.667		0.40	0.57/1.93
	4 : 1	0.517		0.32	0.18/1.02
Co^{2+}/Cu^{2+}	1 : 1	0.632		0.39	0.48/1.65
	4 : 1	0.585		0.34	0.19/1.35
Fe^{2+}/Cu^{2+}	1 : 1	0.700		0.46	0.07/2.17
	4 : 1	0.680		0.44	0.12/2.14
$Na^+/Zn^{2+}/Pb^{2+}/Cu^{2+}$	1 : 1 : 1 : 1	0.706		0.47	0.00/0.14/0.07/2.00
	4 : 4 : 4 : 1	0.692		0.45	0.00/0.006/0.26/2.47

**Table 4** Stability constant (in log K of M–L complex) of heavy metal ions (M) with DETA (L)

Heavy metal ions	Stability constant (log K)[32]
Cu^{2+}	15.9 ± 0.1
Fe^{2+}	6.23
Co^{2+}	8.0 ± 0.2
Ni^{2+}	10.5
Pb^{2+}	8.50
Zn^{2+}	8.80

3.6 Desorption experiments

Desorption efficiency was an important parameter in evaluating the reusability of the adsorbents. In this study, HNO$_3$ was used as the desorption agent. Fig. 9 showed the desorption efficiency of ACF–Cu at different concentrations of HNO$_3$. The desorption efficiency increased as the HNO$_3$ concentration gradually increased. When HNO$_3$ concentration was higher than 0.5 mol L^{-1}, the desorption efficiency almost kept constant and reached the maximum value of 93%. Therefore, 0.5 mol L^{-1} HNO$_3$ was suitable for the desorption of copper ions.

3.7 Repeated use experiments

In order to examine the repeated use performance of the ACF prepared in this study, we have carried out the 6-cycle adsorption–desorption–regeneration experiments for the copper ions,
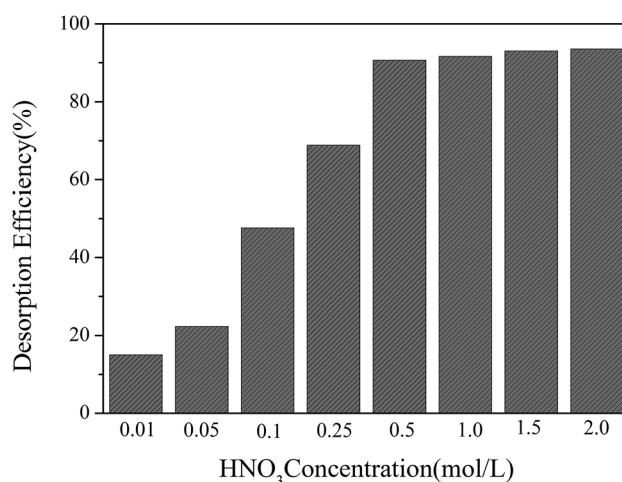
Fig. 9 Desorption efficiency of ACF–Cu samples with different HNO$_3$ concentrations.
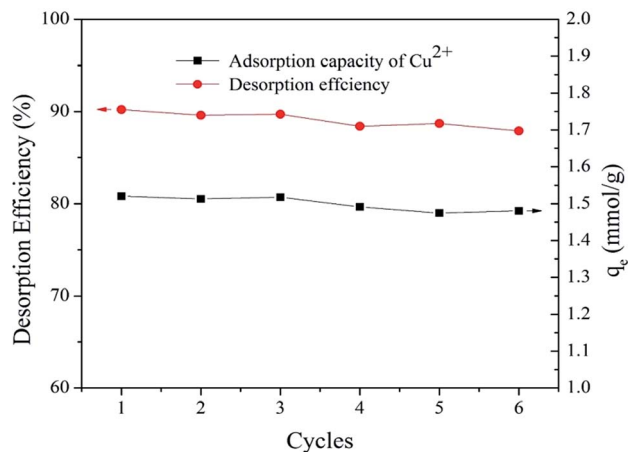
Fig. 10 The copper ion desorption efficiency and adsorption capacity of ACF samples in six adsorption–desorption–regeneration cycles.

and the results were shown in Fig. 10. Both the adsorption capacity and the desorption efficiency were examined in Fig. 10, in an effort to comprehensively evaluate the repeated use performance of the ACF. The results showed that only a slight decrease occurred for both the adsorption capacity and the desorption efficiency during the six cycles, which demonstrated the good repeated use performance of the ACF for the application of copper ion removal.

4. Conclusions

In this paper, the functional cotton fiber (denoted as aminated cotton fiber, ACF), was prepared and used for the detection and adsorption of copper ions in solutions. XPS results indicated that copper ion was mainly complexed with amine groups of the ACF sample. The maximum adsorption capacity for copper ions on ACF sample was 1.84 mmol g^{-1}, as obtained from the Langmuir isotherm model fitting. The copper ion adsorption kinetics with ACF in solutions with different initial copper ion concentrations was best described by the pseudo-second-order (PSO) kinetics model, indicating that chemical adsorption played a dominant role in the adsorption process. A linear relationship, which was used for the determination of copper ion concentrations, was established between the absorbance of ACF–Cu and the copper ion initial concentrations, with a correlation coefficient (R^2) of 0.9962. Besides, the ACF sample also showed great adsorption selectivity to copper ions, and the presence of Na$^+$, Pb^{2+}, Zn^{2+} or Fe^{2+} showed no significant influence on the absorbance of ACF–Cu and the adsorption capacity of the ACF sample. Therefore, the ACF prepared in this study exhibited great practical potential for the simple detection and enhanced adsorption of copper ions in waters and wastewaters.

Acknowledgements

References

1 V. Desai and S. G. Kaler, Role of copper in human neurological disorders, *Am. J. Clin. Nutr.*, 2008, **88**, 855–858.

2 Y. Yu, J. G. Shapter and R. Popelka-Filcoff, Copper removal using bio-inspired polydopamine coated natural zeolites, *J. Hazard. Mater.*, 2014, **273**, 174–182.

3 H. D. Ozsoy and H. Kumbur, Absorption of Cu(II) ions on cotton boll, *J. Hazard. Mater.*, 2006, **136**, 911–916.

4 W. Yantasee, Y. Lin, G. E. Fryxell, K. L. Alford, B. J. Busche and C. D. Johnson, Selective removal of copper(II) from aqueous solutions using fine-grained activated carbon functionalized with amine, *Ind. Eng. Chem. Res.*, 2004, **43**, 2759–2764.

5 K. Thirugnanasambandham and V. Sivakumar, An eco-friendly approach for copper(II) ion adsorption onto cotton seedcake and its characterization: simulation and validation, *J. Taiwan Inst. Chem. Eng.*, 2015, **50**, 1–7.

6 D. W. O'Connell, C. Birkinshaw and T. F. O'Dwyer, Heavy metal adsorbents prepared from the modification of cellulose: a review, *Bioresour. Technol.*, 2008, **99**, 6709–6724.

7 J. C. Y. Ng, W. H. Cheung and G. McKay, Equilibrium studies of the sorption of Cu(II) ions onto chitosan, *J. Colloid Interface Sci.*, 2002, **255**, 64–74.

8 N. Li, R. Bai and C. Liu, Enhanced and selective adsorption of mercury ions on chitosan beads grafted with polyacrylamide *via* surface-initiated atom transfer radical polymerization, *Langmuir*, 2005, **21**, 11780–11787.

9 J. Yang, Y. Wang and T. Tang, Synthesis and adsorption properties for metal ions of mesocyclic diamine grafted chitosan-crown ether, *J. Appl. Polym. Sci.*, 2000, **75**, 1255–1260.

10 Y. Zhu, A. Iton, T. Umemura, H. haraguchi, K. Inagaki and K. Chiba, Determination of REEs in natural water by ICP-MS with the aid of an automatic column changing system, *J. Anal. At. Spectrom.*, 2010, **25**, 1253–1258.

11 P. Li, X. Duan, Z. Chen and Y. Liu, A near-infrared fluorescent probe for detecting copper(II) with high selectivity and sensitivity and its biological imaging applications, *Chem. Commun.*, 2011, **47**, 7755–7757.

12 X. X. Liu, X. J. Liu, M. L. Tao and W. Q. Zhang, A highly selective and sensitive recyclable colorimetric Hg^{2+} sensor based on the porphyrin functionalized polyacrylonitrile fiber, *J. Mater. Chem. A*, 2015, **3**, 13254–13262.

13 C. Liu, X. Liang, J. Liu, Y. Liu, J. Luo and H. Zhu, Efficient removal of Cd(II) ions from aqueous solution *via* visible capturing, *RSC Adv.*, 2016, **6**, 38430–38436.

14 T. Hajeeth, K. Vijayalakshmi, T. Gomathi, P. N. Sudha and S. Anbalagan, Adsorption of copper(II) and nickel(II) ions from aqueous solution using graft copolymer of cellulose extracted from the sisal fiber with acrylic acid monomer, *Compos. Interfaces*, 2014, **21**, 75–86.

15 C. Liu, X. Liang, J. Liu, X. Lei and X. Zhao, Preparation of the porphyrin-functionalized cotton fiber for the chromogenic detection and efficient adsorption of Cd^{2+} ions, *J. Colloid Interface Sci.*, 2017, **488**, 294–302.

16 M. Monier, M. A. Akl and W. M. Ali, Modification and characterization of cellulose cotton fibers for fast extraction of some precious metal ions, *Int. J. Biol. Macromol.*, 2014, **66**, 125–134.

17 W. D. Schecher and D. C. Mcavoy, *MINEQL+: Chemical Equilibrium Modeling System, Version 4.5 for Windows, Environmental Research Software*, Hallowell, ME, 2003.

18 C. Liu, X. Liang, J. Liu and W. Yuan, Desorption of copper ions from the polyamine-functionalized adsorbents: behaviors and mechanisms, *Adsorpt. Sci. Technol.*, 2016, **34**, 455–468.

19 C. Yuan, M. Cui and L. Feng, Efficient removal of Cu(II) using amino-functionalized superparamagnetic nanoparticles prepared *via* SI-ATRP, *J. Appl. Polym. Sci.*, 2015, **1**, 42859.

20 E. Yavuz, G. Bayramoglu, B. F. Şenkal and M. Yakup Arıca, Poly(glycidylmethacrylate) brushes generated on poly(VBC) beads by SI-ATRP technique: hydrazine and amino groups functionalized for invertase adsorption and purification, *J. Chromatogr. B: Anal. Technol. Biomed. Life Sci.*, 2009, **877**, 1479–1486.

21 F. Tang, L. Zhang and Z. Zhang, Cellulose filter paper with antibacterial activity from surface-initiated ATRP, *J. Macromol. Sci., Part A: Pure Appl. Chem.*, 2009, **26**, 989–996.

22 S. Deng, Y. Zheng, F. Xu, B. Wang, J. Huang and G. Yu, Highly efficient sorption of perfluorooctane sulfonate and perfluorooctanoateon a quaternized cotton prepared by atom transfer radical polymerization, *Chem. Eng. J.*, 2012, **193**, 154–160.

23 B. Debora, M. Giancarlo, D. L. Piero, M. Luisa, C. Donatella and V. Crescenzi, Versatile grafting of polysaccharides in homogeneous mild conditions by using atom transfer radical polymerization, *Biomacromolecules*, 2006, 7, 2154–2161.

24 A. Friebe and M. Ulbricht, Controlled pore functionalization of poly(ethylene terephthalate) track-etched membranes *via* surface-initiated atom transfer radical polymerization, *Langmuir*, 2007, **23**, 10316–10322.

25 C. Liu, R. Bai and L. Hong, Diethylenetriamine-grafted poly(glycidyl methacrylate) adsorbent for effective copper ion adsorption, *J. Colloid Interface Sci.*, 2006, **303**, 99–108.

26 Y. Zheng, S. Deng, L. Niu, F. Xu, M. Chai and G. Yu, Functionalized cotton *via* surface-initiated atom transfer radical polymerization for enhanced sorption of Cu(II) and Pb(II), *J. Hazard. Mater.*, 2011, **192**, 1401–1408.

27 Y. Tang, Q. Ma, Y. Luo, L. Zhai, Y. Che and F. Meng, Improved synthesis of a branched poly(ethylene imine)-modified cellulose-based adsorbent for removal and recovery of Cu(II) from aqueous solution, *J. Appl. Polym. Sci.*, 2013, **129**, 1799–1805.

28 Y. Yu, B. N. Murthy, J. G. Shapter, K. T. Constantopoulos, N. H. Voelcker and A. V. Ellis, Benzene carboxylic acid derivatized graphene oxide nanosheets on natural zeolites as effective adsorbents for cationic dye removal, *J. Hazard. Mater.*, 2013, **260**, 330–338.

29 W. Chouyyok, Y. Shin, J. Davidson, W. D. Samuels, N. H. Lafemina, R. D. Rutledge and G. E. Fryxell, Selective removal of copper(II) from natural waters by nanoporous sorbents functionalized with chelating diamines, *Environ. Sci. Technol.*, 2010, **44**, 6390–6395.

30 J. Kim, A. J. Leong, L. F. Lindoy, J. Kim, J. Nachbaur, A. Nezhadali, G. Rounaghi and G. Wei, Metal–ion recognition. Competitive bulk membrane transport of transition and post transition metal ions using oxygen–nitrogen donor macrocycles as ionophores, *J. Chem. Soc., Dalton Trans.*, 2000, **19**, 3453–3459.

31 C. V. Diniz, V. S. T. Ciminelli and F. M. Doyle, The use of the chelating resin Dowex M-4195 in the adsorption of selected heavy metal ions from manganese solutions, *Hydrometallurgy*, 2005, **78**, 147–155.

32 R. M. Smith and A. E. Martell, *Critical Stability Constants*, Springer, Amines, 1975, vol. 2.